Interactions of oral permeation enhancers with lipid membranes in simulated intestinal environments

Larsen, Nanna Wichmann; Kostrikov, Serhii; Hansen, Morten Borre; Hjørringgaard, Claudia Ulrich; Larsen, Niels Bent; Andresen, Thomas Lars; Kristensen, Kasper

Published in:
International Journal of Pharmaceutics

Link to article, DOI:
10.1016/j.ijpharm.2024.123957

Publication date:
2024

Document Version
Publisher's PDF, also known as Version of record

International Journal of Pharmaceutics 654 (2024) 123957

Contents lists available at ScienceDirect

International Journal of Pharmaceutics

journal homepage: www.elsevier.com/locate/ijpharm

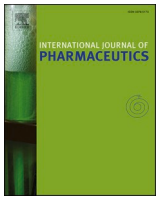

Interactions of oral permeation enhancers with lipid membranes in simulated intestinal environments

Nanna Wichmann Larsen, Serhii Kostrikov, Morten Borre Hansen, Claudia Ulrich Hjørringgaard, Niels Bent Larsen, Thomas Lars Andresen *, Kasper Kristensen *

DTU Health Tech, Department of Health Technology, Technical University of Denmark, 2800 Kgs. Lyngby, Denmark
Center for Intestinal Absorption and Transport of Biopharmaceuticals, Technical University of Denmark, 2800 Kgs. Lyngby, Denmark

ARTICLE INFO

Keywords:
Oral drug delivery
Peptide drugs
Permeation enhancers
Simulated intestinal fluid
Lipid membranes
Membrane activity

ABSTRACT

The oral bioavailability of therapeutic peptides is generally low. To increase peptide transport across the gastrointestinal barrier, permeation enhancers are often used. Despite their widespread use, mechanistic knowledge of permeation enhancers is limited. To address this, we here investigate the interactions of six commonly used permeation enhancers with lipid membranes in simulated intestinal environments. Specifically, we study the interactions of the permeation enhancers sodium caprate, dodecyl maltoside, sodium cholate, sodium dodecyl sulfate, melittin, and penetratin with epithelial cell-like model membranes. To mimic the molecular composition of the real intestinal environment, the experiments are performed with two peptide drugs, salmon calcitonin and desB30 insulin, in fasted-state simulated intestinal fluid. Besides providing a comparison of the membrane interactions of the studied permeation enhancers, our results demonstrate that peptide drugs as well as intestinal-fluid components may substantially change the membrane activity of permeation enhancers. This highlights the importance of testing permeation enhancement in realistic physiological environments and carefully choosing a permeation enhancer for each individual peptide drug.

1. Introduction

Upon being swallowed, oral drugs enter the gastrointestinal tract. From here, the drugs may cross the epithelial cells lining the tract to enter into the circulatory system; see Fig. 1A-C. However, the size and hydrophilic nature of peptide drugs generally limit their diffusion across the epithelial cell layer (Brayden et al., 2020). This constitutes one of the main obstacles for oral peptide drug delivery.

To increase oral peptide bioavailability, permeation enhancers (PEs) are commonly used (Maher et al., 2016; Berg et al., 2022a). Exemplifying this, Rybelsus, a clinically approved oral formulation of the peptide semaglutide, relies on the PE salcaprozate sodium (SNAC) to enhance bioavailability (Drucker, 2020; Berg et al., 2022a) by shifting the peptide towards a monomeric state, reducing peptidase degradation, and increasing epithelial cell membrane permeability (Buckley et al., 2018). Likewise, Mycapssa, a clinically approved oral formulation of the peptide octreotide, is based on the transient permeation enhancement technology, which solubilizes the peptide in an oily suspension with the PE sodium caprylate (C_8) and thereby increases paracellular peptide transport (Tuvia et al., 2014; Berg et al., 2022a).

Together with SNAC, sodium caprate (C_{10}) is the PE tested most extensively in humans (Halberg et al., 2019; Twarog et al., 2019). Mechanistic studies demonstrated that C_{10} can increase membrane fluidity (Yoon et al., 2017; Tran et al., 2023), which may lead to increased transcellular transport across the gastrointestinal epithelium (Maher et al., 2009a). C_{10}-induced membrane perturbations may also alter intracellular processes and, thereby, lead to opening of tight junctions and enhanced paracellular transport (Twarog et al., 2019). Like SNAC and C_{10}, many other PEs may increase cell membrane permeability (Maher et al., 2016). In fact, most PEs are surfactants, which means that they have a high propensity for interacting with cell membranes (Maher et al., 2023). Interactions likely begin via insertion of PE monomers into the membranes. Like in the case of C_{10}, this may alter the packing and fluidity of the membranes (Maher et al., 2016). Accumulation of the PEs on the outer membrane leaflets may also lead to asymmetric membrane expansion, which can induce mechanical stress on the membranes and cause the formation of transmembrane pores (Heerklotz, 2008). At higher concentrations, the PEs may even have a solubilizing effect on the membranes (Lichtenberg et al., 2013). The exact mode of membrane interaction differs between individual PEs,

* Corresponding authors at: DTU Health Tech, Department of Health Technology, Technical University of Denmark, 2800 Kgs. Lyngby, Denmark.
E-mail addresses: tlan@dtu.dk (T.L. Andresen), kakri@dtu.dk (K. Kristensen).

https://doi.org/10.1016/j.ijpharm.2024.123957
Received 19 November 2023; Received in revised form 17 February 2024; Accepted 28 February 2024
Available online 29 February 2024

depending on factors like the spontaneous curvature and the transmembrane flip-flop rate of the PEs (Lichtenberg et al., 2013). Micelles or other self-assembled aggregates formed by the PEs may also play an important mechanistic role. Specifically, self-assembled PE structures may reduce the availability of the PE monomers for inserting into the membranes (Maher et al., 2016), but at the same time, the self-assembled structures may potentially also solubilize lipids or larger fragments dissociating from the membranes (Maher et al., 2021). All in all, this means that PEs may exert a multitude of different effects on lipid membranes. These effects are evidently important for the efficiency and safety of the PEs, yet the interactions of commonly used PEs with lipid membranes are seldom compared. This creates a bottleneck for obtaining a complete and comparative mechanistic understanding of PEs.

Another key aspect of obtaining a full mechanistic understanding is related to the interactions of PEs with peptide drugs (Twarog et al., 2022). For instance, as already mentioned above, SNAC is thought to interact with semaglutide in Rybelsus (Buckley et al., 2018). As another example, it has been reported that the cell-penetrating peptide penetratin and related analogues may form a non-covalent complex with insulin, resulting in increased oral bioavailability of insulin (Nielsen et al., 2014; Diedrichsen et al., 2021). The choice of PE is, however, often based on formulation, manufacturing, and commercial considerations rather than considerations about the peptide drug (Twarog et al., 2019; Brayden et al., 2020), and more studies are needed to elucidate the potential importance of the interactions between PEs and peptide drugs. For example, it is at present not understood whether and how these interactions modify the membrane activity of the PEs.

Along the same lines, PEs may also interact with gastrointestinal fluids (Maher et al., 2019), and especially with the bile salts and phospholipids present in the fluids. In particular, PEs may form mixed micelles with these components (Gradauer et al., 2015; Hossain et al., 2020), and this may, in turn, change the prerequisites for permeation enhancement. Additionally, the intestinal fluid components may alter the interactions between PEs and peptide drugs (Twarog et al., 2022; Hossain et al., 2023). It is, thus, generally thought that intestinal fluid components may impact the efficiency of PEs. However, for most – if not all PEs – it is at present not clear how their interactions with lipid membranes are altered by the intestinal fluid components.

In this study, we used a biophysical approach to investigate the abovementioned mechanistic aspects of permeation enhancement. Specifically, we investigated six common PEs (Maher et al., 2016), namely C_{10} (Maher et al., 2009a, 2009b, 2009c; Halberg et al., 2019; Twarog et al., 2019, 2021, 2022; Drucker, 2020; Tran et al., 2023), dodecyl maltoside (DDM; Gradauer et al., 2015, 2017; Danielsen and Hansen, 2018a), sodium cholate (SC; Danielsen and Hansen, 2018a), sodium dodecyl sulfate (SDS; Anderberg and Artursson, 1993), melittin (Maher et al., 2007a, 2007b, 2009b, 2009c; Danielsen and Hansen, 2018b), and penetratin (Kamei et al., 2008, 2020; Nielsen et al., 2014; Kristensen et al., 2015b; Diedrichsen et al., 2021; Birch et al., 2023); see Fig. 2A. Since peptide translocation across lipid membranes and cells is often related to membrane permeabilization (Wimley, 2010; Trier et al., 2015), we used a calcein release assay to evaluate the membrane permeabilization induced by the PEs; see Fig. 1D. In this assay, the fluorophore calcein is encapsulated at high, self-quenching concentrations in synthetic lipid vesicles (LVs). If the membranes of the LVs are permeabilized, calcein will be released, leading to an increased fluorescence emission (Allen and Cleland, 1980; Lee, 2018). To explore the effects of peptide drugs on the membrane interactions of the PEs, we performed the experiments both without and with the two peptide drugs salmon calcitonin (sCT) and desB30 human insulin; see Fig. 2B. Likewise, to evaluate the effect of intestinal fluid components on the action of the PEs, we conducted the experiments in both a simple phosphate buffer and in fasted-state simulated intestinal fluid (FaSSIF). To further elucidate the observed intermolecular interactions, dynamic light scattering (DLS) and Nile red fluorescence were used as complimentary techniques. In the former technique, temporal fluctuations in light scattering intensity provide information about the size of molecular assemblies in solutions, whereas in the latter technique, the fluorescence intensity of the small fluorophore Nile red correlates with the presence of hydrophobic environments, such as the ones formed by micelles (Sackett and Wolff, 1987; Rusanov et al., 2022). Overall, our results provide a broad, systematic comparison of the membrane interactions of the investigated PEs. Of particular importance, our data demonstrate that these interactions may be significantly altered by both peptide drugs and intestinal fluid components. These fundamental insights may be of importance for future oral peptide formulations.

2. Materials and methods

2.1. Materials

Calcein, Nile red, sodium dihydrogen phosphate, sodium chloride

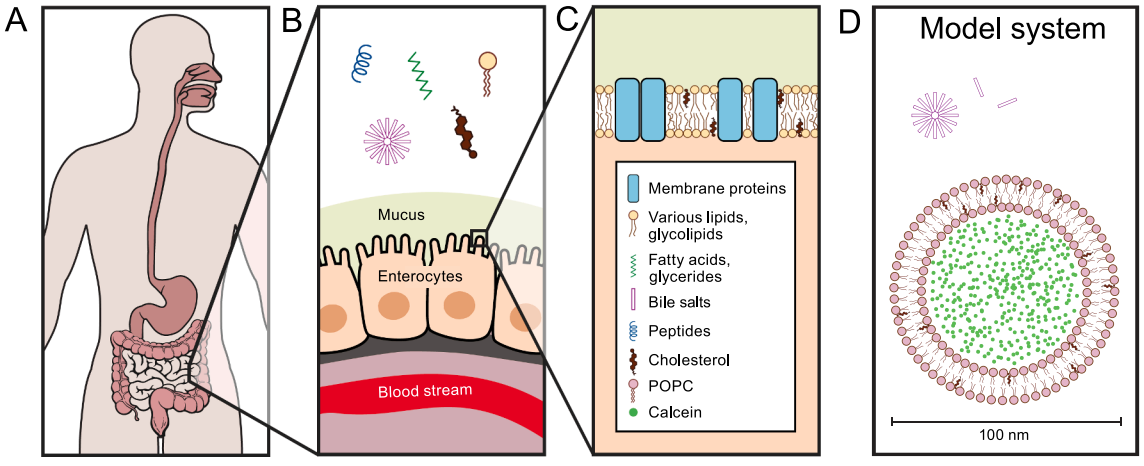

Fig. 1. Absorption route of oral peptide drugs. (A) Upon being swallowed, tablets and capsules with peptide drugs enter the gastrointestinal tract. (B) The peptide drugs have to cross the epithelial cell layer to be absorbed into the circulatory system. Absorption often occurs via transcellular transport, which involves peptide translocation across the epithelial cell membrane. The absorption process is commonly thought to start from the intestinal fluid having a complex composition of bile salts, fatty acids, glycerides, and lipids. (C) The cell membranes consist of membrane proteins and different lipid types, including cholesterol and phosphatidylcholine. (D) In the present study, POPC:cholesterol (9:1) lipid vesicles (LVs) containing dissolved calcein at a self-quenching concentration were used as a minimal model system of epithelial cell membranes. To mimic the intestinal molecular environment, some experiments were performed in fasted-state simulated intestinal fluid (FaSSIF).

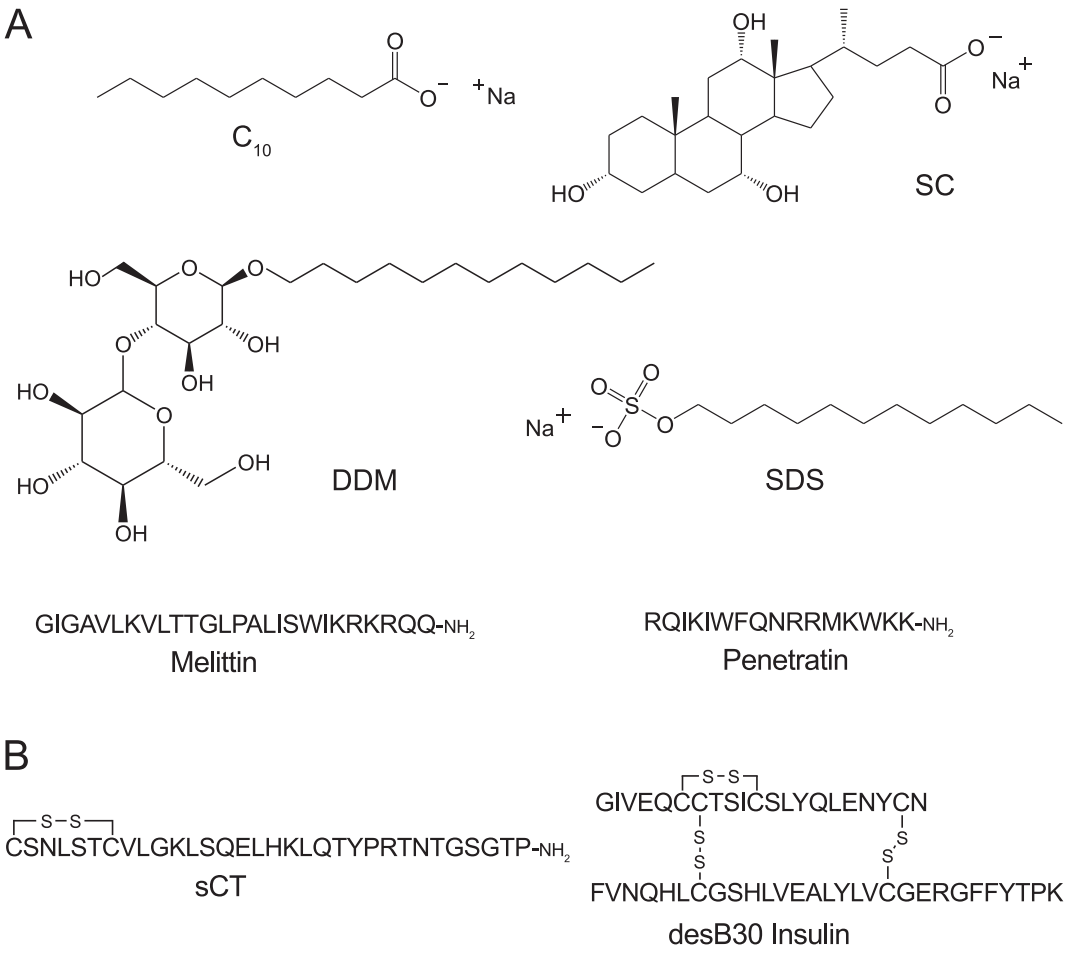

Fig. 2. Structures and sequences of PEs and peptide drugs. (A) PEs. (B) Peptide drugs. The small-molecule PEs are shown as chemical structures, and the peptides are shown by one-letter amino acid sequences. Peptide disulfide bridges are shown by -S-S-, and C-terminal amidations are shown by $–NH_2$.

(NaCl), sodium hydroxide (NaOH), Triton X-100, sodium dodecyl sulfate (SDS), *n*-dodecyl-β-D-maltoside (DDM), sodium cholate hydrate (SC), sodium caprate (C_{10}), *tert*-butanol, dimethyl sulfoxide (DMSO), piperidine, dimethylformamide (DMF), dichloromethane (DCM), hexafluoroisopropanol (HFIP), iodine (I_2), isopropanol, diethyl ether, trifluoroacetic acid (TFA), triisopropylsilane (TIPS), and acetonitrile (MeCN) were purchased from Sigma-Aldrich (St. Louis, MO, USA). 1-Palmitoyl-2-oleoyl-*sn*-glycero-3-phosphocholine (POPC) and cholesterol from ovine wool were purchased from Avanti Polar Lipids (Alabaster, AL, USA). Slurry for preparing Sepharose CL-4B columns was purchased from GE Healthcare (Little Chalfont, UK). Econo-Column glass chromatography column (dimensions 1.5 × 20 cm) was purchased from Bio-Rad (Hercules, CA, USA). Q-Max syringe filters with 0.22-μm and 0.45-μm cellulose acetate filtration membranes were purchased from Frisenette (Knebel, Denmark). Black, untreated, flat-bottomed Nunc F96 microwell polystyrene plates were purchased from Thermo Fischer Scientific (Waltham, MA, USA). Salcaprozate sodium (SNAC) was purchased from Vulcanchem (Pasadena, CA, USA). The desB30 human insulin was kindly provided by Novo Nordisk A/S (Måløv, Denmark). Fmoc-protected amino acids (including the special Fmoc protected amino acids Fmoc-L-Leu-L-Ser[PSI(Me, Me)Pro]–OH, Fmoc-L-Glu-OtBu, and Fmoc-L-Asp-OtBu), ethyl cyanohydroxyiminoacetate (oxyma) and *N*,*N*′-diisopropylcarbodiimide (DIC) were purchased from Iris Biotech (Marktredwitz, Germany). Resin was purchased from Rapp Polymere (Tübingen, Germany). Water (H_2O) was prepared using a Milli-Q Academic water purification system (Millipore, Burlington, MA, USA) to have a resistivity of 18.2 MΩ•cm.

2.2. Synthesis and purification of peptides

Melittin, penetratin, and salmon calcitonin (sCT) were synthesized using standard solid-phase peptide synthesis, as previously described (Wichmann et al., 2022). All peptides were synthesized on an Initiator+ Alstra microwave-assisted peptide synthesizer (Biotage, Uppsala, Sweden). A TentaGel S RAM resin (loading 0.23 mmol/g) was used for melittin and sCT, and an Fmoc-PAL-AM resin (loading 0.61 mmol/g) was used for penetratin. Fmoc-deprotection was performed by treating the resin twice with deprotection solution (20 % piperidine, 0.1 M oxyma in DMF). For melittin and penetratin, this was done for 2 min followed by 5 min at 75 °C, and for sCT, this was done for 30 sec followed by 2 min at 75 °C. The resin was washed four-five times with DMF. Coupling of amino acids was performed by adding amino acid solution (4–5 eq. of Fmoc-L-amino acid-OH, 4–5 eq. oxyma, 0.3–0.5 M concentration in DMF) and DIC solution (4–5 eq., 2 M DIC in DMF) before heating the mixture to 75 °C for 10 min for melittin and penetratin, and for 5 min for sCT. Every amino acid was double-coupled by draining the resin, adding fresh reagents, and repeating the coupling as described above. After the coupling reactions, the resin was washed four times with DMF. Extended coupling times were applied for Fmoc-L-Arg (Pbf)–OH and Fmoc-L-Leu-L-Ser[PSI(Me, Me)Pro]–OH; these amino acids were coupled at room temperature for 25 min followed by 75 °C for 5 min. Fmoc-removal on Asp residues was performed with 5 % piperidine rather than 20 %. For histidine residues, the temperature was lowered to 50 °C.

For sCT, after the final coupling, the resin was washed five times with DMF and five times with DCM. Then, to form the disulfide bond, an

iodine solution (1:4 of HFIP/1% I_2 in DCM) was added to the resin, shaken for 2 min, filtered, and washed once with a 1:1 HFIP/DCM solution. The resin was then left to shake for 15 min with a 1:1 HFIP/DCM solution. The solution was drained, and the resin was washed five times with DCM and five times with DMF. Next, Fmoc was removed by adding 20 % piperidine, 0.1 % oxyma in DMF, and the tube was shaken for 2 × 20 min at room temperature.

After deprotection of the final amino acid residue, the resin was washed five times with DMF, five times with DCM, and air dried. Alternatively, the resin was washed with DMF, DCM, DMF, DCM, isopropanol, DCM, and diethyl ether. The resin was then treated with cleavage cocktail (95 % TFA, 2.5 % H_2O, 2.5 % TIPS for melittin and penetratin; 90 % TFA, 5 % H_2O, 5 % TIPS for sCT) for 4 h. The crude peptide was precipitated in cold diethyl ether, centrifuged, and decanted. The crude peptide was purified by RP-HPLC on a Dionex Ultimate 3000 system equipped with an RQ variable wavelength detector and an automated fraction collector, for melittin and penetratin using a Gemini NX 5u, C18, 110 Å, 250 mm × 30 mm column (Phenomenex, Torrance, CA, USA), and for sCT using a Gemini NX 5u, C18, 110 Å, AXIA, 250 mm x 21 mm column (Phenomenex). Both columns were eluted at a flow rate of 20 mL/min. The mobile phases were (A) 0.1 % TFA in H_2O and (B) 0.1 % TFA in MeCN. Pure fractions were combined and lyophilized. Peptides were analyzed on a Nexera X2 RP-HPLC system equipped with LC-30AD pumps, an SIL-30AC autosampler, a CTO-20AC column oven and a PDA detector monitoring at 214 nm, 280 nm, and 492 nm (Shimadzu, Kyoto, Japan) using an XBridge BEH C18, 2.5 μm 3.0 x 150 mm XP column (Waters, Milford, MA, USA) at a flow rate of 0.5 mL/min. RP-HPLC gradients were run using a solvent system consisting of solution A (0.1 % TFA, 5 % MeCN in H_2O) and B (0.1 % TFA in MeCN). Peptide masses were confirmed using an Acquity Ultra Performance UPLC equipped with a Qda detector and an Acquity UPLC BEH C18, 1.7 μm, 2.1 × 50 mm column (Waters) for melittin and penetratin, and an electrospray ionization (ESI) micrOTOF-Q III (Bruker Daltonics, Bremen, Germany) for sCT. The final purities were 99 % for melittin, 93 % for penetratin, and 98 % for sCT as determined by RP-HPLC. The RP-HPLC chromatogram and mass identification for sCT are shown in Figs. S1 and S2; the same data has been published elsewhere for melittin and penetratin (Wichmann et al., 2022).

2.3. Aqueous solutions

Three aqueous solutions were used in the present study: (i) Phosphate buffer with 10 mM phosphate, 100 mM NaCl, pH adjusted to 6.7 using NaOH, osmolality 190 ± 5 mOsmol/kg. The pH, osmolarity and buffer capacity of the phosphate buffer was similar to those of the upper small intestine (Fuchs et al., 2015). (ii) Calcein solution with 60 mM calcein, 10 mM phosphate, pH adjusted to 6.7 using NaOH, osmolality 190 ± 5 mOsmol/kg. The osmolarity of the calcein solution was chosen to match that of the phosphate buffer. The solution was filtered using a 0.22-μm membrane prior to use. (iii) Fasted-state simulated intestinal fluid (FaSSIF) prepared by dissolving FaSSIF powder (Biorelevant, London, UK) in phosphate buffer, resulting in a final solution with 3 mM taurocholate, 0.75 mM phospholipids in phosphate buffer, osmolality 200 ± 2 mOsmol/kg. FaSSIF solutions were equilibrated for at least 2 h before use, and they were used for experiments within 48 h of preparation.

2.4. Preparation of lipid vesicles (LVs)

To obtain a minimalistic model of epithelial cell membranes, lipid vesicles (LVs) were prepared with POPC/cholesterol in a 9:1 molar ratio (Sampaio et al., 2011). To prepare the LVs, the lipids were first dissolved in *tert*-butanol:H_2O (9:1). The *tert*-butanol:H_2O was removed by lyophilization overnight. A calcein solution was then added to the lipids to a final lipid concentration of 50 mM. The resulting lipid suspension was gently vortexed seven times with 5-min intervals between each vortexing before being subject to five freeze–thaw cycles by alternately submerging the sample vial into a liquid nitrogen bath and a 70 ℃ water bath. Next, the lipid suspension was extruded 21 times through a 100-nm polycarbonate membrane (Whatman, GE Healthcare) using a mini-extruder (Avanti Polar Lipids). Non-encapsulated calcein was removed and exchanged by phosphate buffer using a Sepharose CL-4B size-exclusion chromatography column (dimensions 1.5 × 20 cm, phosphate buffer flow rate 1 mL/min). The eluted LVs were added to an Amicon Ultra-4 30 kDa centrifugal filter unit (Merck, Darmstadt, Germany) and concentrated by centrifuging at 2000*g*.

The lipid concentration was determined using RP-HPLC. For this purpose, a Nexera i-series HPLC (Shimadzu) equipped with a PDA and a SEDEX LT-ELSD 100LT evaporative light scattering detector (Sedere, Alfortville, France) together with an Xterra C8 column (Waters) was used with a flow rate of 1 mL/min. The mobile phases were (A) 0.1 % TFA, 5 % MeCN in H_2O and (B) 0.1 % TFA in MeCN. The recorded area under the curve was compared to a POPC standard curve. The total lipid concentration was then calculated by dividing the POPC concentration with 0.9 to take into account that the LVs contained 10 % cholesterol.

The size and monodispersity of the LVs were confirmed using dynamic light scattering (DLS). For this purpose, the LVs were diluted to a lipid concentration of 50 μM in phosphate buffer and then investigated at room temperature using the equipment described below.

2.5. Preparation of solutions with peptides and small-molecule permeation enhancers (PEs)

Peptides and small-molecule permeation enhancers (PEs) were dissolved in either phosphate buffer or FaSSIF, which had been filtered using a 0.22-μm or a 0.45-μm membrane prior to use. The absorption spectra of the peptide solutions were measured using a NanoDrop 2000c spectrophotometer (NanoDrop Products, Thermo Fisher Scientific), and the peptide concentrations were then calculated using Lambert-Beer's law and the following extinction coefficients at 280 nm: 5500 M^{-1} cm^{-1} for melittin, 11000 M^{-1} cm^{-1} for penetratin, 6335 M^{-1} cm^{-1} for desB30 insulin, and 1615 M^{-1} cm^{-1} for sCT (Pace et al., 1995). The concentrations of the small-molecule PEs C_{10}, DDM, SC, SDS, and SNAC were estimated based on weight.

MQuant universal pH-indicator strips (Merck) were used to test whether the PEs changed the pH of the phosphate buffer. Within the concentration range used in our experiments, DDM, SC, SDS, and melittin did not lead to any observable changes in the pH value of the buffer. Up to a concentration of 5 g/L, C_{10} did not lead to any observable changes in the pH of the buffer either, but at concentrations of 20 g/L and 60 g/L, this PE increased the pH value to ~8.0 and ~8.5, respectively. However, since most of our experiments were done at a C_{10} concentration of 5 g/L, this effect was not ascribed any significant importance for the interpretation of our data. At a concentration of 1.5 g/L, penetratin slightly decreased the pH of the phosphate buffer to ~6.0, but since this concentration is 3-fold higher than the maximal penetratin concentration used in our experiments and only a small change in pH was recorded, this effect was not ascribed any importance either.

2.6. Calcein release assay

Solutions with PEs and/or peptide drugs in phosphate buffer or FaSSIF were transferred to black 96-well plates. The plates were heated to 37 °C. Then, solutions with LVs, also preheated to 37 °C, were added to the wells. The final PE and peptide drug concentrations in the wells were variable, the final lipid concentration of the LVs in the wells was 50 μM, and the final sample volume was 150 μL. Due to the addition of the LVs, the final samples with FaSSIF were diluted 1:9 with phosphate buffer. Upon adding the LVs, all samples were immediately mixed by multipipette. Kinetic measurements were initiated within 20 s of adding the LVs. The fluorescence intensity, *F*, was measured using a Spark multimode microplate reader (Tecan, Männedorf, Switzerland) with an

excitation wavelength of 491 nm and an emission wavelength of 514 nm. The temperature was kept at 37 °C throughout the experiments.

The calcein release was calculated using the equation

$$\text{Calcein release } (\%) = \frac{F - F_0}{F_{max} - F_0} \times 100\%$$

where F_0 is the fluorescence intensity of intact LVs, measured using LVs added to phosphate buffer or FaSSIF, and F_{max} is the maximum fluorescence intensity, measured from LVs in phosphate buffer or FaSSIF treated with 0.5 % Triton X-100. In the kinetic measurement for DDM shown in Fig. 3C, an abrupt 10 % decrease in the fluorescence intensity occurred during the measurement; this was ascribed to an accidental movement of the plate, and accordingly, the presented curve has been corrected for this effect.

2.7. Dynamic light scattering (DLS)

Dynamic light scattering (DLS) was performed on a Zetasizer Nano ZS (Malvern, Worcestershire, UK). The prepared samples were incubated for 30 min at 37 °C before investigation. The temperature was also kept at 37 °C when measuring. Measurements with LVs were generally performed using a lipid concentration of 50 μM. The acquired data were analyzed using an intensity-based size-distribution analysis. Average size distributions from multiple measurements were created using the instrument software. The light-scattering intensity was evaluated through the derived photon count rate, which was calculated by dividing the measured count rate with the transmission percentage of the laser attenuator.

2.8. Nile red assay

All samples were mixed in black 96-well plates to a final volume of 100 μL. 2 μL of 1.5 mM Nile red in DMSO was added to each of the wells to a final Nile red concentration of 29 μM. The solutions were mixed by pipette and incubated at 37 °C for at least 30 min before transfer to the Spark multimode microplate reader. The Nile red fluorescence emission intensity of the samples at 633 nm was then measured using an excitation wavelength of 550 nm while keeping the temperature at 37 °C.

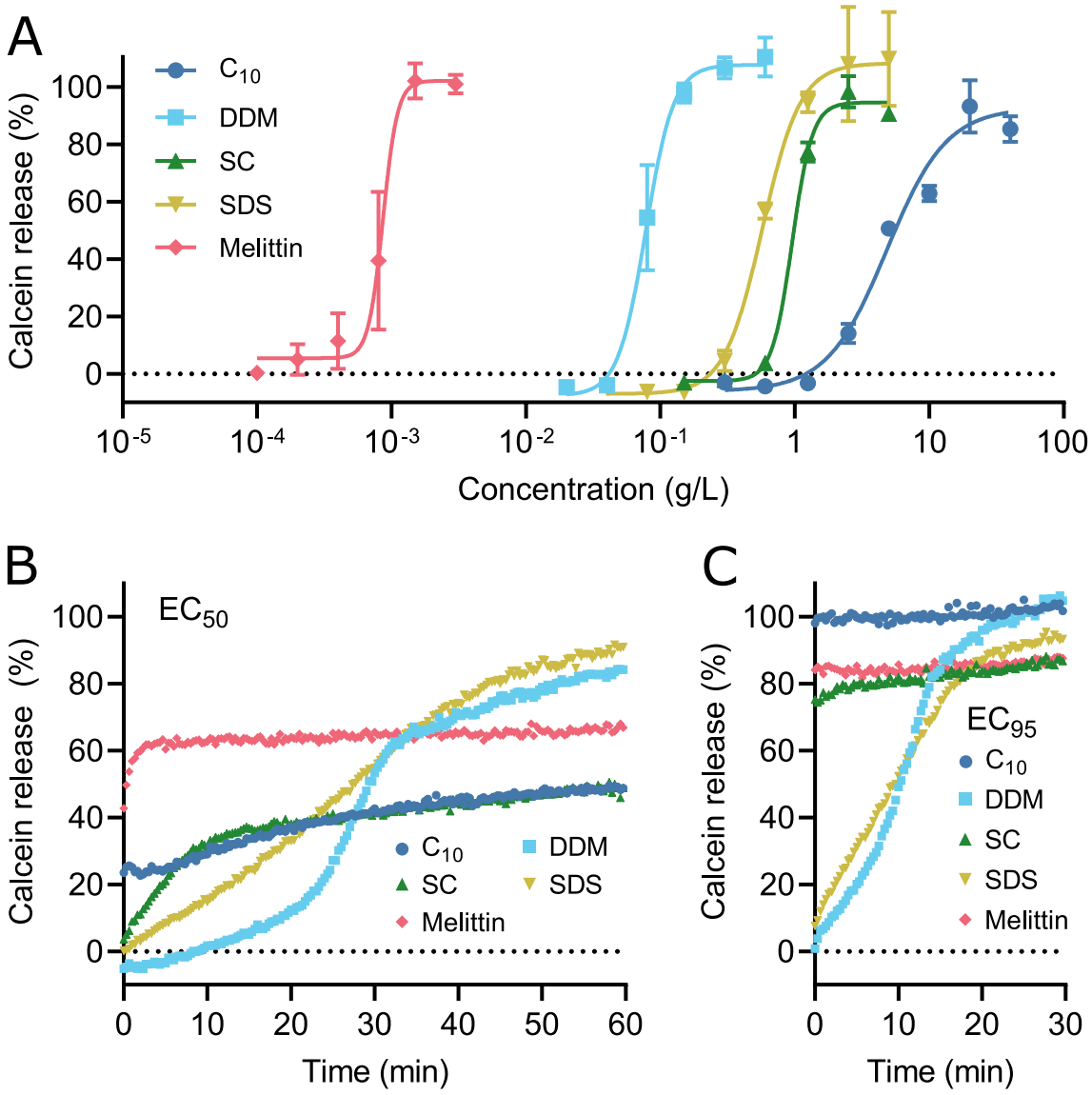

Fig. 3. Calcein release from POPC/cholesterol (9:1) LVs incubated with PEs in phosphate buffer. (A) Calcein release induced by varying concentrations of PEs upon 30 min incubation. (B,C) Calcein release kinetics at EC_{50} (B) and EC_{95} (C). In Panel A, the data are the average of three separate measurements, except the C_{10} data point at 20 g/L, which is the average of six separate measurements. The error bars represent the standard deviations. In Panels B and C, the data show example curves based on single measurements.

2.9. Statistical analysis

The statistical analysis was done using a two-tailed *t*-test. To take into account that the compared samples could have unequal variances, the test was done using Welch's correction. The analysis was performed using Prism (GraphPad Software, Boston, MA, USA).

3. Results and discussion

3.1. Interactions of PEs with lipid membranes

We performed the calcein release assay using POPC/cholesterol (9:1) LVs, which provide a simplistic mimic of epithelial cell membranes (Sampaio et al., 2011). We first evaluated the lipid-membrane interactions of the PEs in phosphate buffer (10 mM phosphate, 100 mM NaCl, pH 6.7). Specifically, PEs at varying concentrations were mixed with the LVs in the phosphate buffer, and the calcein release was measured after 30 min. We initially aimed to perform this experiment not only with the six mentioned PEs, but also with SNAC. We found, however, that SNAC precipitated over time in the phosphate buffer, and due to this reason, we excluded SNAC from our experiments. Interestingly, limited aqueous solubility and gradual precipitation of SNAC has also been reported elsewhere, albeit in simulated intestinal fluids (Twarog et al., 2022). Penetratin did not result in any calcein release; see Fig. S3. This is in agreement with previous reports that this peptide does not disrupt membranes without anionic lipids (Thorén et al., 2000; Kauffman et al., 2015). The data for the rest of the PEs are shown in Fig. 3A. All of the PEs caused full calcein release at sufficiently high concentrations. This emphasizes the point that a key feature of many PEs is the ability to interact with and disrupt lipid membranes. As exemplified by previous studies on C_{10}, these interactions may not only lead to transcellular transport but also paracellular transport (Brayden et al., 2015; Twarog et al., 2019, 2021).

To compare the PEs, we determined the concentrations that gave rise to 50 % and 95 % of the maximal calcein signal after 30 min incubation in phosphate buffer using a sigmoidal fit. These concentrations, here termed EC_{50} and EC_{95}, respectively, are shown in Table 1. Melittin was by far the most potent membrane disruptor of the investigated PEs. This reflects previous reports in the literature that this membrane-active peptide is a highly effective pore former (Matsuzaki et al., 1997, Lee et al., 2013). Of the small-molecule PEs, DDM was found to give calcein release at a lower concentration than the other compounds. Oppositely, C_{10} required a higher concentration to release calcein from the LVs. Interestingly, the recorded EC_{50} values seem to be in fair agreement with data obtained for Caco-2 cells across different studies, that is, C_{10}, DDM, SDS, and melittin were found to induce transcellular macromolecular flux at concentrations of ~2 g/L, ~3×10^{-1} g/L, ~1×10^{-1} g/L, and ~3×10^{-3} g/L, respectively (Anderberg and Artursson, 1993; Maher et al., 2007a, 2009a; Gradauer et al., 2015; Twarog et al., 2020). This again emphasizes the fundamental importance of understanding the interactions of PEs with lipid membranes. To a certain extent, our results also correlate to data from ex vivo and in situ models, although it is clear that direct comparison to these models is more complicated: In the case of C_{10}, macromolecular transport across isolated jejunal and colonic mucosae was induced at concentrations of ~2-4 g/L (Maher et al., 2009a, 2009b; Twarog et al., 2021), which is close to the EC_{50}. A ~5-10-fold higher concentration of C_{10} was required to obtain a similar effect in intestinal and colonic instillation and closed loop models (Maher et al., 2009a, 2009c; Berg et al., 2022b). Melittin was reported to induce transepithelial macromolecular flux across isolated colonic mucosae at a concentration of ~5×10^{-2} g/L (Maher et al., 2009b) and in jejunal and colonic instillation models at a concentration of ~1×10^{-1} g/L (Maher et al., 2009c). On the one hand, these concentrations are ~50-100-fold higher than the EC_{50}, but on the other hand, they are still much lower than the concentration determined for C_{10} to induce a similar effect. That melittin was found to require a higher concentration for permeation enhancement ex vivo and in situ than in vitro may be related to binding to the mucus (Maher et al., 2007b) and enzymatic degradation (Lundquist and Artursson, 2016). In the case of DDM, macromolecular transepithelial flux was induced at concentrations of ~0.5-1 g/L in isolated colonic mucosae and in colonic closed loop models (Petersen et al., 2012; Gradauer et al., 2015), that is, this PE was found to be effective in colonic tissue at concentrations that are about 10-fold higher than the EC_{50}. The same PE was, however, largely inefficient in jejunal tissue (Petersen et al., 2012). That DDM was found to have an effect in colonic but not in jejunal tissue could have to do with regional differences in apical membrane susceptibility to surfactants (Petersen et al., 2012), but the fact that the actions of C_{10} and melittin are less dependent on the gut region could also suggest that varying membrane interactions of the individual PEs may explain their differing effects on intestinal and colonic tissue.

To further examine this point, the calcein release kinetics were measured for each of the PEs at their EC_{50} and EC_{95}. At EC_{50}, C_{10} and melittin induced a rapid but limited burst of calcein release; in contrast, DDM, SC, and SDS induced a somewhat slower release; see Fig. 3B. At EC_{95}, the calcein release by SC was quicker than at EC_{50}, but DDM and SDS still induced slow release; see Fig. 3C. In agreement with these observations, melittin was previously reported to induce rapid membrane permeabilization (Schwarz et al., 1992), whereas DDM and SDS were reported to act slowly on membranes, possibly due to slow flipping to the inner membrane leaflet (Lichtenberg et al., 2013). Taken together, this demonstrates that there are clear differences in the membrane interaction kinetics of the various PEs.

The differences in calcein release kinetics may well reflect different membrane interaction modes of the PEs (Heerklotz, 2008). To further scrutinize this point, we used DLS to measure the size of the LVs upon 30 min incubation with the PEs at EC_{95}. The recorded size distributions are shown in Fig. 4, and the light-scattering intensities are shown in Fig. S4. SC, melittin, and penetratin did not give significant changes in neither the intensity of the scattered light nor the size of the LVs. Supported by previous reports, this suggests that SC and melittin induced calcein release through localized membrane pores (Kokkona et al., 2000; Kristensen et al., 2015a), and that penetratin did not lead to any structural remodeling of the membrane (Thorén et al., 2000). There were seemingly also still intact LVs remaining in the presence of SDS, but the overall intensity of the scattered light decreased ~10-fold and an additional peak around 5 nm emerged. This indicates a decrease in the number of intact LVs and the formation of mixed SDS-lipid micelles (Juan-Colás et al., 2020). Along the same lines, C_{10} led to ~30-fold decrease in the intensity of the scattered light and the emergence of a new peak at ~4 nm, again suggesting the disintegration of the LVs and the creation of mixed C_{10}-lipid micelles. Finally, DDM also gave a ~15-fold decrease in the intensity of the scattered light and an altered size distribution, implying the eradication of the LVs and the creation of mixed, heterogenous structures with a mean size around 40 nm (Lambert et al., 1998). Measurements with the fluorophore Nile red imply that C_{10}, DDM, and SDS form micelles or other self-assembled aggregates at or close to the EC_{50}; see Fig. S5. Although the formation of such self-assembled structures may limit the amount of PE monomers available for interaction with the membranes, the fact that the calcein

Table 1
PE concentrations giving 50 % and 95 % of the maximal calcein signal from POPC/cholesterol (9:1) LVs upon 30 min incubation in phosphate buffer. The concentrations are termed EC_{50} and EC_{95}, respectively.

	EC_{50} (g/L)	EC_{95} (g/L)
C_{10}	5.0	22
DDM	7.6×10^{-2}	1.6×10^{-1}
SC	9.5×10^{-1}	1.6
SDS	5.7×10^{-1}	1.5
Melittin	8.6×10^{-4}	1.2×10^{-3}

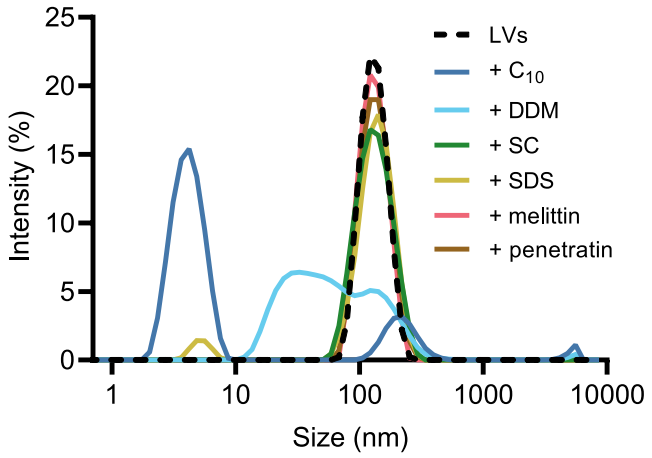

Fig. 4. DLS measurements of POPC/cholesterol (9:1) LVs upon incubation for 30 min in phosphate buffer with PEs at EC_{95}. Since no EC_{95} was recorded for penetratin, a concentration of 0.5 g/L was used for this PE. For reference, an experiment with the LVs only was also performed. The recorded data were evaluated using an intensity-based size-distribution analysis. The shown size distributions are the average of two separate measurements.

release increased as a function of PE concentration in parallel with the formation of the self-assembled structures suggests that the free PE monomers that were removed from solution due to membrane binding were replenished by new monomers released by the self-assembled structures (Maher et al., 2016). Alternatively, it could be that the membrane permeabilization induced by C_{10}, DDM, and SDS not only involved the action of monomers on the membranes, but also extraction of lipids or membrane fragments from the LVs to the self-assembled structures (Maher et al., 2021). For completeness, it should be emphasized that the membrane interaction mode of the PEs may also depend on their concentration. Specifically, some surfactants may induce local transmembrane pore formation at lower concentrations and membrane solubilization at higher concentrations (Lichtenberg et al., 2013). Some membrane-active peptides may exhibit the same behavior (Henriksen and Andresen, 2011). However, in the present study, we did not consider the effect of concentration on the mode of membrane interaction any further. Overall, it is evident that the investigated PEs may disrupt lipid membranes with highly variable kinetics and via fundamentally different mechanisms. This could have a profound effect on both the effectiveness and safety of the PEs, although this point is not commonly considered in the literature.

3.2. The effect of peptide drugs on the interactions of PEs with lipid membranes

To cast light on the impact of interactions between PEs and peptide drugs, we measured calcein release from the POPC/cholesterol (9:1) LVs incubated for 30 min in phosphate buffer in the presence of the various PEs at their EC_{50} in the absence or presence of the two peptide drugs sCT and insulin. These two peptide drugs are positively and negatively charged, respectively, at the pH of the phosphate buffer; consequently, they provide ample opportunity for electrostatic interactions with both positively and negatively charged PEs.

Under the conditions described above, the peptide drugs on their own did not lead to any calcein release in the absence of PEs. However, the peptide drugs altered the calcein release of several of the PEs; see Fig. 5. Specifically, C_{10} induced more calcein release in the presence of either of the peptide drugs, and SC induced more calcein release in the presence of sCT. On the contrary, the effect of SDS was diminished in the presence of insulin. The calcein release of the rest of the PEs was not significantly altered by the peptide drugs.

To investigate the molecular interactions that led to these results, we next used DLS. For reference, we first determined the size of sCT and insulin in the phosphate buffer to be 3.3 ± 0.6 nm and 4.9 ± 1.5 nm, respectively; see Fig. S6. These sizes indicate that both peptides form small oligomeric structures in the phosphate buffer (Hosoya et al., 2004). Having estimated the size of the peptide drugs in the phosphate buffer, we next evaluated the size distribution of the PEs at their EC_{50} in the absence or presence of the peptide drugs. C_{10} without peptide drugs yielded a high light-scattering intensity and formed large, heterogenous structures; see Figs. 6 and S7. The average size of the structures was 70 nm, as estimated from a number-based size-distribution analysis. These structures were likely vesicular (Namani and Walde, 2005; Maher et al., 2009a; Berg et al., 2022b). Addition of the peptide drugs to the C_{10} vesicles only resulted in minor changes in the light-scattering intensity but still led to a certain reorganization of the vesicles. For sCT, the reorganization of the vesicles is further substantiated by an increased Nile red fluorescence intensity; see Fig. S8. It is possible that the peptide-induced restructuring of the vesicles shifted the equilibrium towards more monomeric C_{10} and that this was the driver for the increased calcein release. Another explanation for the increased calcein release could be that C_{10} bound to positively charged residues in the two peptides, forming hydrophobic ion pairs (Ristroph and Prud'homme, 2019). Such hydrophobization of the peptides could potentially lead to increased peptide-membrane interactions and, thereby, cause membrane permeabilization and calcein release (Trier et al., 2015).

For DDM, SC, SDS, and melittin, the light-scattering intensity was low both without or with the peptide drugs, and except in the case of DDM, the size-distribution analyses did not reveal any structural remodeling; see Figs. S6 and S7. Likewise, mixing of the mentioned PEs with the peptide drugs did not lead to any marked changes in Nile red fluorescence intensity; see Fig. S8. Like in the case of C_{10}, hydrophobic ion pairing could provide a plausible explanation for the effects observed in the calcein release experiments, that is, the increased calcein release of SC in the presence of sCT could be related to enhanced membrane interactions of the hydrophobized peptide, whereas the decreased effect of SDS in the presence of insulin could be related to lower availability of SDS due to binding to insulin. The hypothesis on hydrophobic ion pairing is further supported by previous reports that sodium deoxycholate – which is structurally similar to SC – can form hydrophobic ion pairs with sCT (Yoo and Park, 2004) and that SDS can form hydrophobic ion pairs with insulin (Griesser et al., 2017). In the case of SDS, though, it is also possible that the decreased activity in the

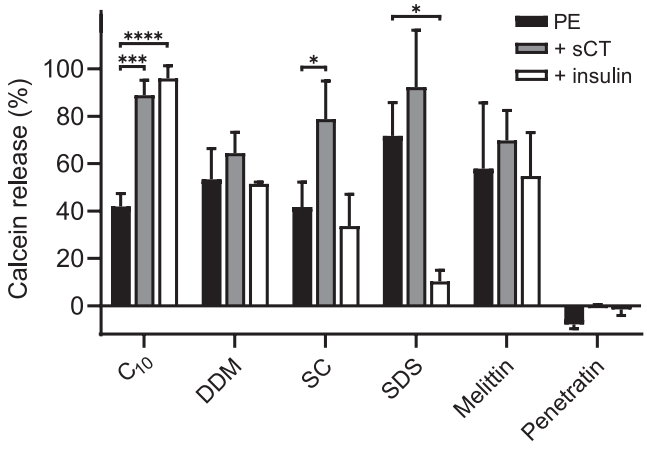

Fig. 5. Calcein release from POPC/cholesterol (9:1) LVs upon incubation for 30 min in phosphate buffer with PEs at EC_{50} without or with 0.3 g/L peptide drug. Since no EC_{50} was recorded for penetratin, a concentration of 0.5 g/L was used for this PE. The data are the average of at least three separate measurements, except the data for penetratin, which are the average of two separate measurements. The error bars show the standard deviations. ✱: $p < 5 \times 10^{-2}$, ✱✱✱: $p < 5 \times 10^{-4}$, ✱✱✱✱: $p < 5 \times 10^{-5}$.

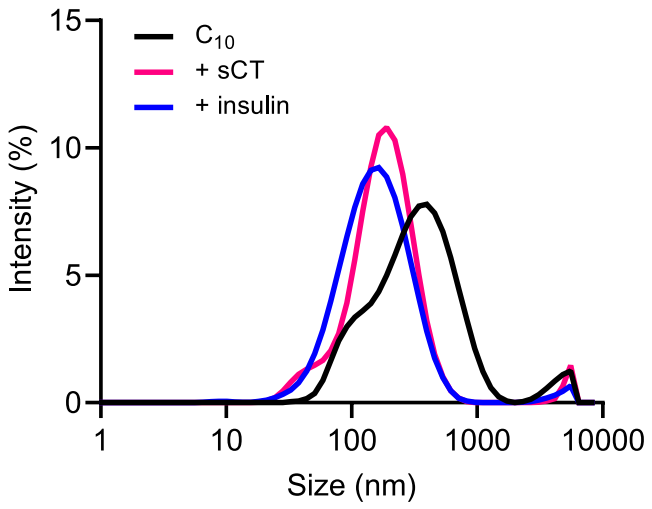

Fig. 6. DLS measurements of C_{10} at EC_{50} upon incubation for 30 min in phosphate buffer without or with 0.3 g/L peptide drug. The recorded data were evaluated using an intensity-based size-distribution analysis. The shown size distributions are the average of two separate measurements.

calcein release assay had to do with structural reorganization of the SDS micelles due to insertion of insulin into the micelles, that is, an altered structure of the SDS micelles could alter the availability of SDS for interacting with the LVs, or alternatively, the propensity of the micelles for solubilizing lipids or membrane fragments released from the LVs.

For penetratin alone or in the presence of sCT, the light-scattering intensity was low, but mixing of penetratin with insulin led to a dramatic increase in the scattering intensity and the occurrence of large aggregates of > 500 nm; see Figs. S6 and S7. These aggregates were only associated with a small increase in Nile red signal; see Fig. S8. This suggests that formation of these aggregates is driven not by the hydrophobic effect but rather by electrostatic interactions between the negatively charged insulin and the positively charged penetratin. To confirm this hypothesis, we performed an experiment in which 7 mg/L penetratin was incubated with 0.6 g/L insulin in phosphate buffer; these conditions led to visible precipitates in the sample. When performing the same experiment with a phosphate buffer containing 1 M NaCl, there was no precipitation, likely due to increased ionic screening and, thereby, reduced electrostatic interactions in the high-salt buffer. It is thus evident that insulin and penetratin can form large electrostatically stabilized aggregates, consistent with previous findings (Kristensen et al., 2015b). The observation that these aggregates may precipitate raises a question about the stability of formulations containing insulin together with penetratin or derived analogues, which is particularly important given the widespread use of this type of formulation (Kamei et al., 2008, 2020; Nielsen et al., 2014; Kristensen et al., 2015b; Diedrichsen et al., 2021; Birch et al., 2023). Accordingly, future studies should make sure to document both the short- and long-term stability of insulin/penetratin formulations.

Generally, the presented data clearly demonstrate that peptide drugs may alter the membrane activity of PEs. This, in turn, suggests that mechanistic studies of the PEs should be done in context of specific drugs, that is, it may not be possible to understand the action of a given PE without considering its interplay with different types of drugs.

3.3. The effect of intestinal fluid components on the interactions of PEs with lipid membranes

To evaluate the impact of intestinal fluid components, we performed the calcein release experiments in FaSSIF. This fluid contains 3 mM of the bile salt taurocholate together with 0.75 mM phospholipid in phosphate buffer, thereby providing a simple mimic of the fasted-state intestinal environment (Fuchs et al., 2015). We first tested the temporal calcein release from the POPC/cholesterol (9:1) LVs in FaSSIF, finding only small release within 1 h; see Fig. S9. We then went ahead and measured the calcein release from the LVs after 30 min incubation in FaSSIF with peptide drugs; see Fig. 7A. FaSSIF with insulin did not result in any calcein release, but FaSSIF with sCT caused substantial release. Since FaSSIF contains taurocholate – which has a structure similar to SC and is present at a concentration of 3 mM close to the measured EC_{50} of 2 mM for SC – a possible explanation for the membrane permeabilization induced by sCT is that taurocholate hydrophobizes sCT in a manner similar to that hypothesized for SC. In any case, the observation that FaSSIF causes sCT to permeabilize lipid membranes highlights the importance of studying transepithelial transport of peptide drugs in realistic intestinal environments.

To probe the impact of FaSSIF on the action of the PEs, we then measured calcein release from the LVs incubated for 30 min in FaSSIF with PEs at their EC_{50} without or with peptide drugs. Immediately after preparation, there was visible precipitation in the samples with melittin and penetratin. As taurocholate is negatively charged in FaSSIF while both melittin and penetratin are highly positively charged and contain a lot of hydrophobic residues, the precipitation is likely due to the formation of insoluble hydrophobic ion pairs. This effect may dramatically reduce the availability of the two peptides, potentially limiting their applicability as PEs for oral drug delivery. It is not clear why FaSSIF induced precipitation of melittin and penetratin while SC did not. It is possible that it has to do with differential complexation efficiencies of the charged functional groups on taurocholate and SC with the peptides (Claus et al., 2023), but it could also have to do with intricate hydrophobic interactions between the bile salts, phospholipids and peptides (Hossain et al., 2023). The rest of the PEs remained soluble during the incubation in FaSSIF, allowing us to perform the intended experiments; see Fig. 7B. The calcein release induced by C_{10} in FaSSIF was similar to the calcein release in phosphate buffer. Combining C_{10} with sCT led to a slight increase in calcein release, but contrary to the experiments in phosphate buffer, combining C_{10} with insulin did not alter the calcein release. The calcein release induced by DDM tended to slightly decrease in FaSSIF compared to phosphate buffer. This is in accordance with a previous report that the permeation enhancement by DDM is reduced in FaSSIF (Gradauer et al., 2015). Finally, the calcein release induced by SC increased in FaSSIF, whereas the effect of SDS was eradicated, although there was still substantial calcein release when SDS was combined with sCT. The latter finding may, however, have to do with the actions of sCT alone. Overall, it is evident that PEs as well as peptide drugs may interact with intestinal fluid components, and that this interaction may significantly modify their membrane interactions.

To obtain a better mechanistic understanding, we used DLS to evaluate FaSSIF without or with PEs at their EC_{50}. The recorded size distributions are shown in Fig. 8, and the light-scattering intensities are shown in Fig. S10. For FaSSIF without PEs, the intensity of the scattered light was high, and a single uniform population centered at 46 nm was identified, in agreement with previous reports (Kloefer et al., 2010; Dening et al., 2021). This shows that the taurocholate and phospholipids self-assembled into mixed micelles or other types of colloidal particles. Adding SDS to FaSSIF greatly reduced the light-scattering intensity and led to the emergence of a new peak at 7 nm. This strongly suggests that SDS formed mixed micelles with the taurocholate and phospholipids in FaSSIF. These mixed micelles seemingly diminished the activity of SDS, possibly because they reduced the amount of free SDS available for interacting with the LVs. In contrast to SDS, neither DDM nor SC led to major changes in the light-scattering intensity or the size distribution of FaSSIF. This indicates that these two PEs did not significantly alter the structure of the colloidal particles in the FaSSIF. However, the FaSSIF altered the activity of the two PEs in opposite directions, that is, there was slightly less calcein release for DDM in FaSSIF, whereas there was much more for SC. The reduced activity of DDM may possibly be explained by a lower availability of the monomers due to insertion into

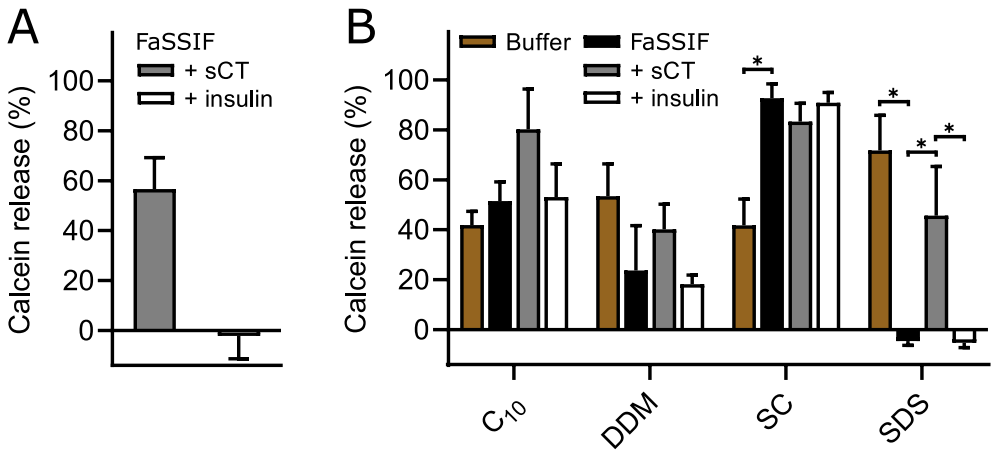

Fig. 7. Calcein release from POPC/cholesterol (9:1) LVs upon incubation for 30 min in FaSSIF. (A) Data for FaSSIF with 0.3 g/L peptide drug. (B) Data for FaSSIF with PEs at EC_{50} without or with 0.3 g/L peptide drug. For reference, data for PEs at EC_{50} in phosphate buffer is also included. In Panel A, the data are the average of three separate measurements, and in Panel B, the data are the average of three or four separate measurements, except the data for FaSSIF with C_{10}/sCT, which are the average of two separate measurements. The error bars show the standard deviations. ✱: $p < 5 \times 10^{-2}$.

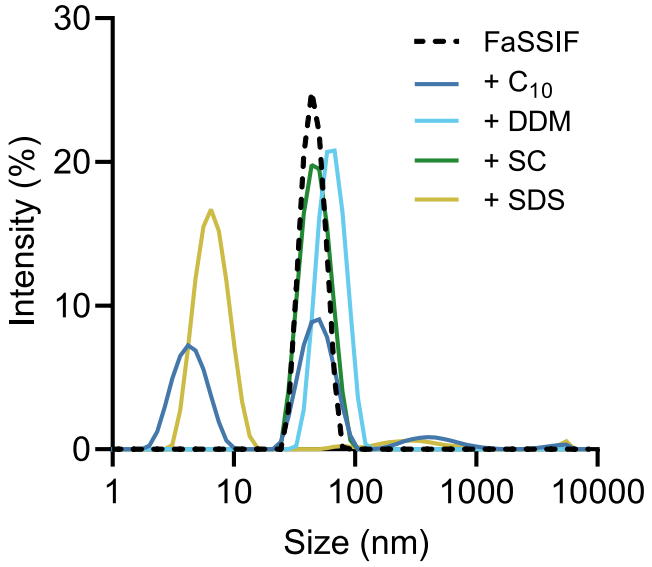

Fig. 8. DLS measurements of FaSSIF without or with PEs at EC_{50} upon 30 min incubation. The recorded data were evaluated using an intensity-based size-distribution analysis. The shown size distributions are the average of two separate measurements, except for the size distribution for C_{10}, which is the average of four separate measurements.

the colloidal particles in the FaSSIF (Gradauer et al., 2015). The increased activity of SC, on the other hand, may occur because SC and the taurocholate in FaSSIF have similar structures with additive effects in the calcein release assay. Finally, the effect of C_{10} was variable, that is, in some measurements C_{10} decreased the light-scattering intensity and led to the formation of mixed micelles of 5 nm, but in other measurements C_{10} did not affect the light scattering intensity or colloidal size distribution of FaSSIF. This suggests that C_{10} causes a cooperative structural reorganization of FaSSIF when its concentration is beyond a threshold value around EC_{50}. It is worth highlighting that this effect did seemingly not alter the membrane permeabilization of C_{10}, in agreement with a previous observation that C_{10} dissolved in buffer or in simulated intestinal fluids exerted a similar permeation-enhancing effect in rat intestines (Berg et al., 2022b).

Taken together, our data demonstrate that PEs may interact directly with intestinal fluid components. This interaction may not only modify the lipid-membrane interactions of the PEs, but potentially also lead to restructuring of the gastrointestinal colloids. Since the interactions of peptide drugs with these colloids can impact both the enzymatic stability and the transport properties of the peptides (Dening et al., 2021), it may be hypothesized that PEs impact oral bioavailability in complex ways beyond their direct interactions with the mucosa and the peptide drugs. For completeness, it should be mentioned that more factors than those considered in the present study may impact the in-vivo activity of PEs. For example, interactions between PEs and the mucus layer covering the epithelium may significantly decrease PE availability (Maher et al., 2007b) or alter the barrier function of the mucus (Mortensen et al., 2022). Also, like peptide drugs, peptide PEs may undergo enzymatic degradation in the gastrointestinal tract (Wang et al., 2015). Nevertheless, we believe that the information put forward in the present work may prove to be useful for the rational development of novel oral peptide dosage forms.

4. Conclusion

PEs for oral drug delivery are generally membrane-active compounds, yet their direct interactions with lipid membranes are rarely studied. In this work, we used the calcein release assay in combination with DLS and Nile red fluorescence to elucidate the lipid-membrane interactions of the six common PEs C_{10}, DDM, SC, SDS, melittin, and penetratin. Except the latter, all of the investigated PEs were found to permeabilize lipid membranes. C_{10}, melittin, and in part SC induced rapid membrane permeabilization, whereas DDM and SDS induced slow permeabilization. SC and melittin likely formed localized pores in the membranes, and C_{10}, DDM, and SDS exerted a solubilizing effect. Interestingly, the concentrations required for membrane disruption correlated well with previously reported concentrations in Caco-2 transport studies and, to a certain extent, also with concentrations used for ex vivo and in situ studies. This emphasizes the mechanistic importance of the interactions between PEs and lipid membranes.

Another important mechanistic aspect of PEs is their interactions with peptide drugs. To cast light on how these interactions affect the membrane activity of the studied PEs, we investigated the effect of adding the two peptide drugs sCT and insulin to our experimental setup. We found that there was more membrane permeabilization by C_{10} in the presence of both sCT and insulin. Likewise, the membrane permeabilization by SC was also increased by sCT, but on other hand, the activity of SDS was reduced by insulin. This shows that the membrane interactions of PEs may be influenced by peptide drugs. It is likely that this, at least in some cases, has to do with hydrophobic ion pairing between the PEs and the peptide drugs. Thus, it may not be possible to

understand the actions of a given PE without considering it in the context of specific drugs.

A third and equally important aspect of PEs is their interactions with components of the gastrointestinal fluids. To scrutinize this point, we performed our experiments in FaSSIF. Melittin and penetratin precipitated in this fluid, but the rest of the PEs remained soluble. The membrane permeabilization by SC increased in FaSSIF, possibly due to an additive effect with the taurocholate in the FaSSIF. In contrast, the membrane permeabilization by SDS and in part DDM decreased in FaSSIF, possibly because these PEs were incorporated into mixed colloidal particles in the fluids. Both C_{10} and SDS were capable of remodulating the FaSSIF colloidal particles altogether. This demonstrates that interactions of PEs with gastrointestinal fluids may lead to myriad different effects. Consequently, future works on PEs should aim to consider the effects of gastrointestinal fluid components on the action of the PEs.

CRediT authorship contribution statement

Nanna Wichmann Larsen: Writing – review & editing, Writing – original draft, Validation, Methodology, Investigation, Formal analysis. **Serhii Kostrikov:** Writing – review & editing, Methodology, Investigation. **Morten Borre Hansen:** Writing – review & editing, Methodology, Investigation. **Claudia Ulrich Hjørringgaard:** Writing – review & editing, Methodology, Investigation. **Niels Bent Larsen:** Writing – review & editing, Supervision, Conceptualization. **Thomas Lars Andresen:** Writing – review & editing, Supervision, Funding acquisition, Conceptualization. **Kasper Kristensen:** Writing – review & editing, Visualization, Supervision, Methodology, Formal analysis, Conceptualization.

Declaration of competing interest

The authors declare that they have no known competing financial interests or personal relationships that could have appeared to influence the work reported in this paper.

Data availability

Data will be made available on request.

Acknowledgements

We thank Jannik Bruun Larsen for providing critical feedback on the manuscript and Nanna Elmstedt Bild for helping with the graphical illustrations. Furthermore, we thank Novo Nordisk A/S for providing desB30 human insulin. Financial support for this work was kindly provided by the Novo Nordisk Foundation grant NNF16OC0022166.

Appendix A. Supplementary material

Supplementary data to this article can be found online at https://doi.org/10.1016/j.ijpharm.2024.123957.

References

Allen, T.M., Cleland, L.G., 1980. Serum-induced leakage of liposome contents. Biochim. Biophys. Acta 597, 418–426.
Anderberg, E.K., Artursson, P., 1993. Epithelial transport of drugs in cell culture. VIII: effects of sodium dodecyl sulfate on cell membrane and tight junction permeability in human intestinal epithelial (Caco-2) cells. J. Pharm. Sci. 82, 392–398.
Berg, S., Edlund, H., Goundry, W.R.F., Bergström, C.A.S., Davies, N.M., 2022a. Considerations in the developability of peptides for oral administration when formulated together with transient permeation enhancers. Int. J. Pharm. 628, 122238.
Berg, S., Kärrberg, L., Suljovic, D., Seeliger, F., Söderberg, M., Perez-Alcazar, M., Van Zuydam, N., Abrahamsson, B., Hugerth, A.M., Davies, N., Bergström, C.A.S., 2022b. Impact of the intestinal concentration and colloidal structure on the permeation-enhancing efficiency of sodium caprate in the rat. Mol. Pharmaceut. 19, 200–212.
Birch, D., Sayers, E.J., Christensen, M.V., Jones, A.T., Franzyk, H., Nielsen, H.M., 2023. Stereoisomer-dependent membrane association and capacity for insulin delivery facilitated by penetratin. Pharmaceutics 15, 1672.
Brayden, D.J., Maher, S., Bahar, B., Walsh, E., 2015. Sodium caprate-induced increases in intestinal permeability and epithelial damage are prevented by misoprostol. Eur. J. Pharm. Biopharm. 94, 194–206.
Brayden, D.J., Hill, T.A., Fairlie, D.P., Maher, S., Mrsny, R.J., 2020. Systemic delivery of peptides by the oral route: formulation and medicinal chemistry approaches. Adv. Drug Deliv. Rev. 157, 2–36.
Buckley, S.T., Bækdal, T.A., Vegge, A., Maarbjerg, S.J., Pyke, C., Ahnfelt-Rønne, J., Madsen, K.G., Schéele, S.G., Alanentalo, T., Kirk, R.K., Pedersen, B.L., Skyggebjerg, R.B., Benie, A.J., Strauss, H.M., Wahlund, P.-O., Bjerregaard, S., Farkas, E., Fekete, C., Søndergaard, F.L., Borregaard, J., Hartoft-Nielsen, M.-L., Knudsen, L.B., 2018. Transcellular stomach absorption of a derivatized glucagon-like peptide-1 receptor agonist. Sci. Transl. Med. 10, eaar7047.
Claus, V., Sandmeier, M., Hock, N., Spleis, H., Lindner, S., Kalb, M., Bernkop-Schnürch, A., 2023. Counterion optimization for hydrophobic ion pairing (HIP): unraveling the key factors. Int. J. Pharm. 647, 123507.
Danielsen, E.M., Hansen, G.H., 2018a. Probing the action of permeation enhancers sodium cholate and N-dodecyl-β-D-maltoside in a porcine jejunal mucosal explant system. Pharmaceutics 10, 172.
Danielsen, E.M., Hansen, G.H., 2018b. Impact of the cell-penetrating peptides (CPPs) melittin and Hiv-1 tat on the enterocyte brush border using a mucosal explant system. Biochim. Biophys. Acta 1860, 1589–1599.
Dening, T.J., Douglas, J.T., Hageman, M.J., 2021. Do macrocyclic peptide drugs interact with bile salts under simulated gastrointestinal conditions? Mol. Pharmaceut. 18, 3086–3098.
Diedrichsen, R.G., Harloff-Helleberg, S., Werner, U., Besenius, M., Leberer, E., Kristensen, M., Nielsen, H.M., 2021. Revealing the importance of carrier-cargo association in delivery of insulin and lipidated insulin. J. Control. Release 338, 8–21.
Drucker, D.J., 2020. Advances in oral peptide therapeutics. Nat. Rev. Drug Discov. 19, 277–289.
Fuchs, A., Leigh, M., Kloefer, B., Dressman, J.B., 2015. Advances in the design of fasted state simulating intestinal fluids: FaSSIF-V3. Eur. J. Pharm. Biopharm. 94, 229–240.
Gradauer, K., Nishiumi, A., Unrinin, K., Higashino, H., Kataoka, M., Pedersen, B.L., Buckley, S.T., Yamashita, S., 2015. Interaction of mixed micelles in the intestine attenuates the permeation enhancing potential of alkyl-maltosides. Mol. Pharmaceutics 12, 2245–2253.
Gradauer, K., Iida, M., Watari, A., Kataoka, M., Yamashita, S., Kondoh, M., Buckley, S.T., 2017. Dodecylmaltoside modulates bicellular tight junction contacts to promote enhanced permeability. Mol. Pharmaceutics 14, 4734–4740.
Griesser, J., Hetényi, G., Moser, M., Demarne, F., Jannin, V., Bernkop-Schnürch, A., 2017. Hydrophobic ion pairing: key to highly payloaded self-emulsifying peptide drug delivery systems. Int. J. Pharm. 520, 267–274.
Halberg, I.B., Lyby, K., Wassermann, K., Heise, T., Zijlstra, E., Plum-Mörschel, L., 2019. Efficacy and safety of oral basal insulin versus subcutaneous insulin glargine in type 2 diabetes: a randomised, double-blind, phase 2 trial. Lancet Diabetes Endocrinol. 7, 179–188.
Heerklotz, H., 2008. Interactions of surfactants with lipid membranes. Q. Rev. Biophys. 41, 205–264.
Henriksen, J.R., Andresen, T.L., 2011. Thermodynamic profiling of peptide membrane interactions by isothermal titration calorimetry: a search for pores and micelles. Biophys. J. 101, 100–109.
Hosoya, O., Chono, S., Saso, Y., Juni, K., Morimoto, K., Seki, T., 2004. Determination of diffusion coefficients of peptides and prediction of permeability through a porous membrane. J. Pharm. Pharmacol. 56, 1501–1507.
Hossain, S., Joyce, P., Parrow, A., Jõemetsa, S., Höök, F., Larsson, P., Bergström, C.A.S., 2020. Influence of bile composition on membrane incorporation of transient permeability enhancers. Mol. Pharmaceutics 17, 4226–4240.
Hossain, S., Kneiszl, R., Larsson, P., 2023. Revealing the interaction between peptide drugs and permeation enhancers in the presence of intestinal bile salts. Nanoscale 15, 19180–19195.
Juan-Colás, J., Dresser, L., Morris, K., Lagadou, H., Ward, R.H., Burns, A., Tear, S., Johnson, S., Leake, M.C., Quinn, S.D., 2020. The mechanism of vesicle solubilization by the detergent sodium dodecyl sulfate. Langmuir 36, 11499–11507.
Kamei, N., Morishita, M., Eda, Y., Ida, N., Nishio, R., Takayama, K., 2008. Usefulness of cell-penetrating peptides to improve intestinal insulin absorption. J. Control. Release 132, 21–25.
Kamei, N., Kawano, S., Abe, R., Hirano, S., Ogino, H., Tamiwa, H., Takeda-Morishita, M., 2020. Effects of intestinal luminal contents and the importance of microfold cells on the ability of cell-penetrating peptides to enhance epithelial permeation of insulin. Eur. J. Pharm. Biopharm. 155, 77–87.
Kauffman, W.B., Fuselier, T., He, J., Wimley, W.C., 2015. Mechanism matters: a taxonomy of cell penetrating peptides. Trends Biochem. Sci. 40, 749–764.
Kloefer, B., van Hoogevest, P., Moloney, R., Kuentz, M., Leigh, M.L.S., Dressman, J., 2010. Study of standardized taurocholate-lecithin powder for preparing the biorelevant media FeSSIF and FaSSIF. Dissolut. Technol. 17, 6–13.
Kokkona, M., Kallinteri, P., Fatouros, D., Antimisiaris, S.G., 2000. Stability of SUV liposomes in the presence of cholate salts and pancreatic lipases: effect of lipid composition. Eur. J. Pharm. Sci. 9, 245–252.
Kristensen, K., Ehrlich, N., Henriksen, J.R., Andresen, T.L., 2015a. Single-vesicle detection and analysis of peptide-induced membrane permeabilization. Langmuir 31, 2472–2483.
Kristensen, M., Franzyk, H., Klausen, M.T., Iversen, A., Bahnsen, J.S., Skyggebjerg, R.B., Foderà, V., Nielsen, H.M., 2015b. Penetratin-mediated transepithelial insulin

permeation: importance of cationic residues and pH for complexation and permeation. AAPS J. 17, 1200–1209.
Lambert, O., Levy, D., Ranck, J.-L., Leblanc, G., Rigaud, J.-L., 1998. A new "gel-like" phase in dodecyl maltoside-lipid mixtures: implications in solubilization and reconstitution studies. Biophys. J. 74, 918–930.
Lee, M.-T., Sun, T.-L., Hung, W.-C., Huang, H.W., 2013. Process of inducing pores in membranes by melittin. Proc. Natl. Acad. Sci. USA 110, 14243–14248.
Lee, M.-T., 2018. Biophysical characterization of peptide-membrane interactions. Adv. Phys. X 3, 1408428.
Lichtenberg, D., Ahyayauch, H., Goñi, F.M., 2013. The mechanism of detergent solubilization of lipid bilayers. Biophys. J. 105, 289–299.
Lundquist, P., Artursson, P., 2016. Oral absorption of peptides and nanoparticles across the human intestine: opportunities, limitations and studies in human tissues. Adv. Drug Deliv. Rev. 106, 256–276.
Maher, S., Feighery, L., Brayden, D.J., McClean, S., 2007a. Melittin as an epithelial permeability enhancer I: investigation of its mechanism of action in Caco-2 monolayers. Pharm. Res. 24, 1336–1345.
Maher, S., Feighery, L., Brayden, D.J., McClean, S., 2007b. Melittin as a permeability enhancer II: in vitro investigations in human mucus secreting intestinal monolayers and rat colonic mucosae. Pharm. Res. 24, 1346–1356.
Maher, S., Leonard, T.W., Jacobsen, J., Brayden, D.J., 2009a. Safety and efficacy of sodium caprate in promoting oral drug absorption: from in vitro to the clinic. Adv. Drug Deliv. Rev. 61, 1427–1449.
Maher, S., Kennelly, R., Bzik, V.A., Baird, A.W., Wang, X., Winter, D., Brayden, D.J., 2009b. Evaluation of intestinal absorption enhancement and local mucosal toxicity of two promoters. I. Studies in isolated rat and human colonic mucosae. Eur. J. Pharm. Sci. 38, 291–300.
Maher, S., Wang, X., Bzik, V., McClean, S., Brayden, D.J., 2009c. Evaluation of intestinal absorption and mucosal toxicity using two promoters. II. rat instillation and perfusion studies. Eur. J. Pharm. Sci. 38, 301–311.
Maher, S., Mrsny, R.J., Brayden, D.J., 2016. Intestinal permeation enhancers for oral peptide delivery. Adv. Drug Deliv. Rev. 106, 277–319.
Maher, S., Brayden, D.J., Casettari, L., Illum, L., 2019. Application of permeation enhancers in oral delivery of macromolecules: an update. Pharmaceutics 11, 41.
Maher, S., Geoghegan, C., Brayden, D.J., 2021. Intestinal permeation enhancers to improve oral bioavailability of macromolecules: reasons for low efficacy in humans. Expert Opin. Drug Deliv. 18, 273–300.
Maher, S., Geoghegan, C., Brayden, D.J., 2023. Safety of surfactant excipients in oral drug formulations. Adv. Drug Deliv. Rev. 202, 115086.
Matsuzaki, K., Yoneyama, S., Miyajima, K., 1997. Pore formation and translocation of melittin. Biophys. J. 73, 831–838.
Mortensen, J.S., Bohr, S.-S.-R., Harloff-Helleberg, S., Hatzakis, N.S., Saaby, L., Nielsen, H. M., 2022. Physical and barrier changes in gastrointestinal mucus induced by the permeation enhancer sodium 8-[(2-hydroxybenzoyl)amino]octanoate (SNAC). J. Control. Release 352, 163–178.
Namani, T., Walde, P., 2005. From decanoate micelles to decanoic acid/dodecylbenzenesulfonate vesicles. Langmuir 21, 6210–6219.
Nielsen, E.J.B., Yoshida, S., Kamei, N., Iwamae, R., Khafagy, E.-S., Olsen, J., Rahbek, U. L., Pedersen, B.L., Takayama, K., Takeda-Morishita, M., 2014. In vivo proof of concept of oral insulin delivery based on a co-administration strategy with the cell-penetrating peptide penetratin. J. Control. Release 189, 19–24.
Pace, C.N., Vajdos, F., Fee, L., Grimsley, G., Gray, T., 1995. How to measure and predict the molar absorption coefficient of a protein. Protein Sci. 4, 2411–2423.
Petersen, S.B., Nolan, G., Maher, S., Rahbek, U.L., Guldbrandt, M., Brayden, D.J., 2012. Evaluation of alkylmaltosides as intestinal permeation enhancers: comparison between rat intestinal mucosal sheets and Caco-2 monolayers. Eur. J. Pharm. Sci. 47, 701–712.
Ristroph, K.D., Prud'homme, R.K., 2019. Hydrophobic ion pairing: encapsulating small molecules, peptides, and proteins into nanocarriers. Nanoscale Adv. 1, 4207–4237.
Rusanov, A.I., Movchan, T.G., Plotnikova, E.V., 2022. Solubilization of Nile red in micelles and protomicelles of sodium dodecyl sulfate. Molecules 27, 7667.
Sackett, D.L., Wolff, J., 1987. Nile red as a polarity-sensitive fluorescent probe of hydrophobic protein surfaces. Anal. Biochem. 167, 228–234.
Sampaio, J.L., Gerl, M.J., Klose, C., Ejsing, C.S., Beug, H., Simons, K., Shevchenko, A., 2011. Membrane lipidome of an epithelial cell line. Proc. Natl. Acad. Sci. USA 108, 1903–1907.
Schwarz, G., Zong, R.-T., Popescu, T., 1992. Kinetics of melittin induced pore formation in the membrane of lipid vesicles. Biochim. Biophys. Acta 1110, 97–104.
Thorén, P.E.G., Persson, D., Karlsson, M., Nordén, B., 2000. The antennapedia peptide penetratin translocates across lipid bilayers – the first direct observation. FEBS Lett. 482, 265–268.
Tran, H., Aihara, E., Mohammed, F.A., Qu, H., Riley, A., Su, Y., Lai, X., Huang, S., Aburub, A., Chen, J.J.H., Vitale, O.H., Lao, Y., Estwick, S., Qi, Z., ElSayed, M.E.H., 2023. In vivo mechanism of action of sodium caprate for improving the intestinal absorption of a GLP1/GIP coagonist peptide. Mol. Pharmaceutics 6, 929–941.
Trier, S., Linderoth, L., Bjerregaard, S., Strauss, H.M., Rahbek, U.L., Andresen, T.L., 2015. Acylation of salmon calcitonin modulates in vitro intestinal peptide flux through membrane permeability enhancement. Eur. J. Pharm. Biopharm. 96, 329–337.
Tuvia, S., Pelled, D., Marom, K., Salama, P., Levin-Arama, M., Karmeli, I., Idelson, G.H., Landau, I., Mamluk, R., 2014. A novel suspension formulation enhances intestinal absorption of macromolecules via transient and reversible transport mechanisms. Pharm. Res. 31, 2010–2021.
Twarog, C., Fattah, S., Heade, J., Maher, S., Fattal, E., Brayden, D.J., 2019. Intestinal permeation enhancers for oral delivery of macromolecules: a comparison between salcaprozate sodium (SNAC) and sodium caprate (C10). Pharmaceutics 11, 78.
Twarog, C., Liu, K., O'Brien, P.J., Dawson, K.A., Fattal, E., Illel, B., Brayden, D.J., 2020. A head-to-head Caco-2 assay comparison of the mechanisms of action of the intestinal permeation enhancers: SNAC and sodium caprate (C10). Eur. J. Pharm. Biopharm. 152, 95–107.
Twarog, C., McCartney, F., Harrison, S.M., Illel, B., Fattal, E., Brayden, D.J., 2021. Comparison of the effects of the intestinal permeation enhancers, SNAC and sodium caprate (C10): isolated rat intestinal mucosae and sacs. Eur. J. Pharm. Sci. 158, 105685.
Twarog, C., Fattal, E., Noiray, M., Illel, B., Brayden, D.J., Taverna, M., Hillaireau, H., 2022. Characterization of the physicochemical interactions between exenatide and two intestinal permeation enhancers: sodium caprate (C10) and salcaprozate sodium (SNAC). Int. J. Pharm. 626, 122131.
Wang, J., Yadav, V., Smart, A.L., Tajiri, S., Basit, A.W., 2015. Toward oral delivery of biopharmaceuticals: an assessment of the gastrointestinal stability of 17 peptide drugs. Mol. Pharmaceutics 12, 966–973.
Wichmann, N., Lund, P.M., Hansen, M.B., Hjørringgaard, C.U., Larsen, J.B., Kristensen, K., Andresen, T.L., Simonsen, J.B., 2022. Applying flow cytometry to identify the modes of action of membrane-active peptides in a label-free and high-throughput fashion. Biochim. Biophys. Acta 1864, 183820.
Wimley, W.C., 2010. Describing the mechanism of antimicrobial peptide action with the interfacial activity model. ACS Chem. Biol. 5, 905–917.
Yoo, H.S., Park, T.G., 2004. Biodegradable nanoparticles containing protein-fatty acid complexes for oral delivery of salmon calcitonin. J. Pharm. Sci. 93, 488–495.
Yoon, B.K., Jackman, J.A., Kim, M.C., Sut, T.N., Cho, N.-J., 2017. Correlating membrane morphological responses with micellar aggregation behavior of capric acid and monocaprin. Langmuir 33, 2750–2759.